



25th ABCM International Congress of Mechanical Engineering October 20-25, 2019, Uberlândia, MG, Brazil

# COB-2019-1949 LOG-CONFORMATION AND SQUARE ROOT-CONFORMATION TRANSFORMATIONS IN HIGH WEISSENBERG NUMBER FLOWS

Beatriz Liara Carreira Analice Costacurta Brandi

Faculdade de Ciências e Tecnologia, Universidade Estadual Paulista "Júlio de Mesquita Filho" beatrizlcarreira@gmail.com; analice.brandi@unesp.br

Laison Junio da Silva Furlan Matheus Tozo de Araujo Leandro Franco de Souza

Instituto de Ciências Matemáticas e de Computação, Universidade de São Paulo laisonfurlan@usp.br, matheustozo@gmail.com, lefraso@icmc.usp.br

Abstract. The High Weissenberg Number Problem (HWNP) consists in the occurrence of numerical instabilities, resulting from a breakdown of the numerical schemes applied in the constitutive equation solution for non-Newtonian fluids. Considering the incompressible two-dimensional Poiseuille flow, whose the mathematical model adopted for the non-Newtonian fluid extra-stress tensor is the Giesekus and the stability analysis is performed by means of Direct Numerical Simulations (DNS). This work aims to present a comparison between two techniques for HWNP solution. These are matrix decompositions of the tensor conformation: one is known as a log-conformation formulation and the other as a square root-conformation.

**Keywords:** Giesekus fluid, Poiseuille flow, log-conformation tensor, square root-conformation tensor.

## 1. INTRODUCTION

The Computational Fluid Dynamics is the area of scientific computing that studies computational methods for simulation of phenomena involving moving fluids (Fortuna, 2012). The viscoelastic fluid flows study is important in Computational Rheology because many materials used in industrial applications behave like fluids viscoelastic. Examples are automotive and aerospace products, various food packaging, beauty products, paints, and many others. These fluids are characterized by having viscous and elastic properties at the same time, which makes it necessary to add a constitutive equation for the non-Newtonian extra-stress tensor.

At the same time, phenomena related to fluid motion can be very complex. The main difficulty lies in the fact that the Navier-Stokes equations are nonlinear partial differential equations, and the mathematical theory of this equations class is not yet sufficiently developed to allow for analytical solutions in general cases.

Even so, despite the remarkable progress in the viscoelastic fluid flows simulation, numerical instability problems have been emerging along with these advances. In particular, a difficulty known as the High Weissenberg Number Problem presents as a major obstacle (Palhares Jr., 2014). This is a numerical phenomenon that leads to instabilities and/or non convergence of the solution.

The main contribution to solving HWNP in Computational Rheology was presented by Fattal and Kupferman (2004, 2005). These authors proposed a reformulation of the constitutive laws that describe non-Newtonian behavior, using a transformation matrix, which represents the instantaneous polymeric "conformation" (or configuration) of a model set "molecules", in which their unitary eigenvectors represent the axes of the polymer conformation and their eigenvalues represent the magnitude of the polymer conformation extent along the eigenvector directions (Afonso *et al.*, 2012).

At first, Fattal and Kupferman (2004) describe a formulation known as log-conformation, which improves the stability of numerical schemes. The use of the logarithmic variable applied to the definite positive conformation tensor drastically changed the view of numerical simulation to HWNP.

From the good properties of conformation tensor, Balci *et al.* (2011) later proposed a square root matrix transformation. Briefly, the idea is that the conformation tensor has a single symmetric square root tensor that satisfies an evolution equation, ensuring the permanence of the definite positive property.

The objective of this work is to compare two different formulations of the same HWNP stabilization technique. Considering the Poiseuille flow stability for Giesekus viscoelastic fluid, analyzed by means Direct Numerical Simulation,

then a numerical study of the log-conformation formulation (Fattal and Kupferman, 2004) was performed in comparison with the formulation square root-conformation (Balci *et al.*, 2011) to demonstrate the relevance of this methodology in Weissenberg high number flows.

## 2. MATHEMATICAL FORMULATION

The flow is assumed to be unsteady, non-Newtonian, two-dimensional and incompressible, without body forces. The conservation of mass (continuity) and conservation of momentum equations governing the flow as follows

$$\nabla \cdot \mathbf{u} = 0,\tag{1}$$

$$\rho \left[ \frac{\partial \mathbf{u}}{\partial t} + \nabla \cdot (\mathbf{u}\mathbf{u}) \right] = \nabla \cdot \boldsymbol{\sigma},\tag{2}$$

where  $\mathbf{u}$  denotes the velocity field, t is the time,  $\rho$  is the fluid density and  $\boldsymbol{\sigma}$  is the total stress tensor, defined by  $\boldsymbol{\sigma} = 2\eta_s\mathbf{D} + \mathbf{T} - p\mathbf{I}$ . In the last equation,  $\eta_s$  is the Newtonian dynamic viscosity,  $\mathbf{D} = \frac{1}{2}(\nabla\mathbf{u} + (\nabla\mathbf{u})^T)$  is the rate of deformation tensor, p is the pressure,  $\mathbf{I}$  is the identy tensor and  $\mathbf{T}$  is the non-Newtonian extra-stress tensor (symmetric), given by  $\mathbf{T} = \begin{bmatrix} T^{xx} & T^{xy} \\ T^{xy} & T^{yy} \end{bmatrix}$ .

In this paper we worked with viscoelastic fluid flow governed by the non-linear Giesekus constitutive equation (Giesekus, 1982), that is given by

$$\mathbf{T} + \lambda \mathbf{T} + \alpha \frac{\lambda}{\eta_p} (\mathbf{T} \cdot \mathbf{T}) = 2\eta_p \mathbf{D}, \tag{3}$$

where  $\eta_p$  is the coefficient of polymeric viscosity,  $\lambda$  is the relaxation-time of the fluid,  $\alpha$  is the mobility parameter that regulates the shear thinning behavior of the fluid ( $0 \le \alpha \le 1$ ),  $\mathbf{T} \cdot \mathbf{T}$  is a tensor product,  $\mathbf{T}$  is the upper-convected derivative. Considering the two-dimensional flow, Eqs. (1)-(3) were non-dimensionalized using the following parameters:  $\mathbf{x} = L\mathbf{x}^*$ ,  $t = \frac{Lt^*}{U}$ ,  $\mathbf{T} = \mathbf{T}^*\rho U^2$ ,  $p = p^*\rho U^2$ ,  $\mathbf{u} = U\mathbf{u}^*$ , where L and U denote length and velocity scales, respectively.

Therefore, omitting the symbol (\*) for convenience the dimensionless equations are

$$\frac{\partial u}{\partial x} + \frac{\partial v}{\partial y} = 0,\tag{4}$$

$$\frac{\partial u}{\partial t} + \frac{\partial (uu)}{\partial x} + \frac{\partial (uv)}{\partial y} = -\frac{\partial p}{\partial x} + \frac{\beta}{Re} \left[ \frac{\partial^2 u}{\partial x^2} + \frac{\partial^2 u}{\partial y^2} \right] + \frac{\partial T^{xx}}{\partial x} + \frac{\partial T^{xy}}{\partial y}, \tag{5}$$

$$\frac{\partial v}{\partial t} + \frac{\partial (uv)}{\partial x} + \frac{\partial (vv)}{\partial y} = -\frac{\partial p}{\partial y} + \frac{\beta}{Re} \left[ \frac{\partial^2 v}{\partial x^2} + \frac{\partial^2 v}{\partial y^2} \right] + \frac{\partial T^{xy}}{\partial x} + \frac{\partial T^{yy}}{\partial y}, \tag{6}$$

$$T^{xx} + Wi\left(\frac{\partial T^{xx}}{\partial t} + \frac{u\partial T^{xx}}{\partial x} + \frac{v\partial T^{xx}}{\partial y} - 2T^{xx}\frac{\partial u}{\partial x} - 2T^{xy}\frac{\partial u}{\partial y}\right) + \alpha \frac{WiRe}{1-\beta}\left(T^{xx^2} + T^{xy^2}\right) = 2\frac{1-\beta}{Re}\frac{\partial u}{\partial x}, \quad (7)$$

$$T^{xy} + Wi\left(\frac{\partial T^{xy}}{\partial t} + \frac{u\partial T^{xy}}{\partial x} + \frac{v\partial T^{xy}}{\partial y} - T^{xx}\frac{\partial v}{\partial x} - T^{yy}\frac{\partial u}{\partial y}\right) + \alpha \frac{WiRe}{1-\beta}\left(T^{xy}\left(T^{xx} + T^{yy}\right)\right) = \frac{1-\beta}{Re}\left(\frac{\partial v}{\partial x} + \frac{\partial u}{\partial y}\right),\tag{8}$$

$$T^{yy} + Wi\left(\frac{\partial T^{yy}}{\partial t} + \frac{u\partial T^{yy}}{\partial x} + \frac{v\partial T^{yy}}{\partial y} - 2T^{xy}\frac{\partial v}{\partial x} - 2T^{yy}\frac{\partial v}{\partial y}\right) + \alpha \frac{WiRe}{1-\beta}\left(T^{xy^2} + T^{yy^2}\right) = 2\frac{1-\beta}{Re}\frac{\partial v}{\partial y}, \quad (9)$$

where the dimensionless parameters  $Re = \frac{\rho UL}{\eta_0}$  and  $Wi = \frac{\rho U}{L}$  are associated with the Reynolds and Weissenberg numbers, respectively. The amount of Newtonian solvent is controlled by the dimensionless solvent viscosity coefficient  $\beta = \frac{\eta_s}{\eta_0}$ , where  $\eta_0 = \eta_s + \eta_p$  denotes the total shear viscosity, and  $\eta_s$  and  $\eta_p$  represent the Newtonian solvent and polymeric viscosities, respectively.

#### 3. KERNEL CONFORMATION TENSOR TRANSFORMATION

An alternative way to describe viscoelastic models use the tensor conformation  $\bf A$ , wich is symmetric and positive definite. In general, we can write the constitutive equation of the tensor conformation  $\bf A$  as (Martins *et al.*, 2015)

$$\frac{\partial \mathbf{A}}{\partial t} + \nabla \cdot (\mathbf{u}\mathbf{A}) = \mathbf{A}\nabla \mathbf{u} + \nabla \mathbf{u}^T \mathbf{A} + \frac{1}{W_i} f(\mathbf{A}) P(\mathbf{A}), \tag{10}$$

where  $f(\mathbf{A})$  is a scalar function and  $P(\mathbf{A})$  is a tensor that depends of  $\mathbf{A}$ , and are defined according to the model used. Also note that the properties of the conformation tensor ensure that it can be diagonalized into

$$\mathbf{A} = \mathbf{O}\boldsymbol{\Lambda}\mathbf{O}^T,\tag{11}$$

where  $\mathbf{O}$  is an orthogonal matrix formed by the eigenvectors of  $\mathbf{A}$  and  $\mathbf{\Lambda}$  is the diagonal matrix of eigenvalues of  $\mathbf{A}$ .

Fattal and Kupferman (2004, 2005) reformulated the velocity gradient and its transpose into a symmetric traceless pure extension component, the tensor **B** that commutes with **A**, and an anti-symmetric pure rotation component, tensor  $\Omega$ . This local decomposition rule for the traceless second-order transpose of velocity gradient tensor was obtained by setting

$$\mathbf{M} = \nabla \mathbf{u}^T = \mathbf{\Omega} + \mathbf{B} + \mathbf{N}\mathbf{A}^{-1},\tag{12}$$

$$\tilde{\mathbf{M}} = \mathbf{O}^T \nabla \mathbf{u}^T \mathbf{O} = \tilde{\mathbf{\Omega}} + \tilde{\mathbf{B}} + \tilde{\mathbf{N}} \Lambda^{-1}, \tag{13}$$

with the tensors  $\tilde{\mathbf{B}}$ ,  $\tilde{\Omega}$  and  $\tilde{\mathbf{N}}$  representing the symmetric and the two anti-symmetric matrices, respectively, used originally by Fattal and Kupferman (2004).

Replacing these decompositions in Eq. (10) gives the action of the deformation field on  $\bf A$  as a composition of a pure rotation  $\bf \Omega$ , and a symmetric volume preserving deformation  $\bf B$  aligned with the principal axes of  $\bf A$  (Fattal and Kupferman, 2004)

$$\frac{\partial \mathbf{A}}{\partial t} + \nabla \cdot (\mathbf{u}\mathbf{A}) = (\mathbf{\Omega}\mathbf{A} - \mathbf{A}\mathbf{\Omega}) + 2\mathbf{B}\mathbf{A} + \frac{1}{Wi}f(\mathbf{A})P(\mathbf{A}). \tag{14}$$

In particular, for the Giesekus model  $f(\mathbf{A})=1$  and  $P(\mathbf{A})=(\mathbf{I}-\mathbf{A})[\mathbf{I}+\alpha(\mathbf{A}-\mathbf{I})]$  and the ratio between the total stress tensor  $\mathbf{T}$  and  $\mathbf{A}$  is given by  $\mathbf{T}=\xi(\mathbf{A}-\mathbf{I})$ , where  $\xi$  is a scalar defined as  $\xi=\frac{1-\beta}{ReWi}$ .

The elaboration of this method takes place basically by two main steps. First, we determine an evolutionary equation for the eigenvalues of matrix A, which can be written as

$$\frac{\partial \mathbf{\Lambda}}{\partial t} + \nabla \cdot (\mathbf{u} \,\mathbf{\Lambda}) = 2\tilde{\mathbf{B}}\mathbf{\Lambda} + \frac{f(\mathbf{\Lambda})}{Wi}P(\mathbf{\Lambda}). \tag{15}$$

Using Eq. (15), the next step is to construct an evolution equation for the kernel function evaluated at  $\Lambda$ . Before that, the kernel function is defined

$$\mathbb{K}(\mathbf{A}) = \mathbf{O}\mathbb{K}(\mathbf{\Lambda})\mathbf{O}^T,\tag{16}$$

where  $\mathbb{K}()$  represents a continuous, invertible and differentiable matrix function. Finally, the evolution equation  $\mathbb{K}(\Lambda)$  is given by

$$\frac{\partial \mathbb{K}(\mathbf{\Lambda})}{\partial t} + \nabla \cdot (\mathbf{u}\mathbb{K}(\mathbf{\Lambda})) = 2\tilde{\mathbf{B}}\mathbf{\Lambda}\mathbf{J} + \frac{f(\mathbf{\Lambda})}{Wi}P(\mathbf{\Lambda})\mathbf{J},\tag{17}$$

where  $\mathbf{J}$  is the gradient matrix, a diagonal matrix of the form  $\mathbf{J} = diag\left(\frac{\partial \mathbb{K}(\lambda_1)}{\partial \lambda_1}, \frac{\partial \mathbb{K}(\lambda_2)}{\partial \lambda_2}\right)$ , in which  $\lambda_1$  and  $\lambda_2$  are the eigenvalues of the conformation tensor  $\mathbf{A}$ .

In conclusion, the evolution equation for  $\mathbb{K}(\mathbf{A})$  can be expressed in tensorial notation as

$$\frac{\partial \mathbb{K}(\mathbf{A})}{\partial t} + \nabla \cdot (\mathbf{u}\mathbb{K}(\mathbf{A})) = \Omega \mathbb{K}(\mathbf{A}) - \mathbb{K}(\mathbf{A})\Omega + 2\mathbb{B} + \frac{1}{Wi}\mathbb{H}, \tag{18}$$

where  $\mathbb B$  and  $\mathbb H$  are symmetric tensors constructed by the orthogonalization of the diagonal tensors  $D_{\mathbb B}$  and  $D_{\mathbb H}$ , respectively. These tensors can be constructed as

$$\mathbb{B} = \mathbf{O}\mathbf{D}_{\mathbb{B}}\mathbf{O}^{T} = \mathbf{O}\tilde{\mathbf{B}}\mathbf{\Omega}\mathbf{J}\mathbf{O}^{T},\tag{19}$$

$$\mathbb{H} = \mathbf{O}\mathbf{D}_{\mathbb{H}}\mathbf{O}^{T} = f(\mathbf{\Lambda})\mathbf{O}P(\mathbf{\Lambda})\mathbf{J}\mathbf{O}^{T}.$$
(20)

# 3.1 Log-conformation

In the log-conformation formulation, the logarithm of the tensor conformation A was defined as the kernel function, that is

$$\mathbf{\Psi} = \mathbb{K}(\mathbf{A}) = \ln(\mathbf{A}),\tag{21}$$

and the inverse kernel function is given by

$$e^{\mathbf{\Psi}} = \mathbf{A}.\tag{22}$$

The calculation starts with an evolution equation for  $\Psi$ , as well as to return to the variable  $\mathbf{A}$ , the tensors  $\Psi$  and  $e^{\Psi}$  were calculated by means of the diagonalization of  $\mathbf{A} = \mathbf{O}\Lambda\mathbf{O}^T$ , that is,  $\Psi = \mathbf{O}ln(\Lambda)\mathbf{O}^T$ , where  $\Lambda$  is the matrix of eigenvalues and  $\mathbf{O}$  is the matrix of eigenvectors.

Also, we can calculate the diagonal gradient matrix J by

$$\mathbf{J} = \frac{\partial \mathbb{K}(\mathbf{\Lambda})}{\partial \mathbf{\Lambda}} = \frac{\partial ln(\mathbf{\Lambda})}{\partial \mathbf{\Lambda}} = \frac{1}{\mathbf{\Lambda}} = \mathbf{\Lambda}^{-1}.$$
 (23)

In conclusion, after appropriate replacements, then  $\Psi = ln(\mathbf{A})$  satisfies the following equation

$$\frac{\partial \mathbf{\Psi}}{\partial t} + \nabla \cdot (\mathbf{u} \, \mathbf{\Psi}) = (\Omega \mathbf{\Psi} - \mathbf{\Psi} \Omega) + 2\mathbf{B} + \frac{f(e^{\mathbf{\Psi}})}{Wi} e^{-\mathbf{\Psi}} P(e^{\mathbf{\Psi}}), \tag{24}$$

where the functions  $f(e^{\Psi})$  and  $P(e^{\Psi})$  are set according to the constitutive model. Thus, we have  $f(e^{\Psi})=1$  and  $P(e^{\Psi})=(\mathbf{I}-e^{\Psi})[\mathbf{I}+\alpha(e^{\Psi}-\mathbf{I})].$ 

## 3.2 Square root-conformation

In the square root-conformation formulation, the kernel function of the tensor conformation A was defined as

$$Q = \mathbb{K}(\mathbf{A}) = \mathbf{A}^{\frac{1}{2}},\tag{25}$$

and the inverse kernel function is given by

$$Q^2 = \mathbf{A}.\tag{26}$$

Again, it is necessary to determine an evolution equation for Q, and then return to the variable A. Therefore, the tensors Q and  $Q^2$  are calculated by means of the diagonalization of  $A = O\Lambda O^T$ , that is,  $Q = O\Lambda^{\frac{1}{2}}O^T$ .

Calculating the diagonal gradient matrix J by

$$\mathbf{J} = \frac{\partial \mathbb{K}(\mathbf{\Lambda})}{\partial \mathbf{\Lambda}} = \frac{\partial \mathbf{\Lambda}^{\frac{1}{2}}}{\partial \mathbf{\Lambda}} = \frac{\mathbf{\Lambda}^{-\frac{1}{2}}}{2} = \frac{1}{2\mathbf{\Lambda}}.$$
 (27)

In conclusion, then  $Q = A^{\frac{1}{2}}$  satisfies the following equation

$$\frac{\partial \mathbf{Q}}{\partial t} + \nabla \cdot (\mathbf{u} \, \mathbf{Q}) = (\Omega \mathbf{Q} - \mathbf{Q}\Omega) + \mathbf{B} \mathbf{Q} + \frac{f(\mathbf{Q}^2)}{2Wi} \mathbf{Q}^{-1} P(\mathbf{Q}^2), \tag{28}$$

where the functions  $f(\mathbf{Q}^2)$  and  $P(\mathbf{Q}^2)$  are set according to the constitutive model. Thus, we have  $f(\mathbf{Q}^2)=1$  and  $P(\mathbf{Q}^2)=(\mathbf{I}-\mathbf{Q}^2)[\mathbf{I}+\alpha(\mathbf{Q}^2-\mathbf{I})]$ .

#### 4. DIRECT NUMERICAL SIMULATION

In order to simplify the problem and eliminate the pressure treatment in the momentum equation, we chose the vorticity-velocity formulation (Brandi *et al.*, 2017). Then, the two-dimensional vorticity  $\omega_z$  is defined by

$$\omega_z = \frac{\partial u}{\partial y} - \frac{\partial v}{\partial x}.\tag{29}$$

By deriving Eq. (29) with respect to x and considering the continuity equation, we obtain a Poisson equation for the v velocity component

$$\frac{\partial^2 v}{\partial x^2} + \frac{\partial^2 v}{\partial y^2} = \frac{\partial \omega_z}{\partial x}.$$
 (30)

Now, deriving the momentum equation in direction y with respect to x and subtracting the derivative of the momentum equation in direction x with respect to y has

$$\frac{\partial \omega_z}{\partial t} + \frac{\partial \omega_z}{\partial x}u + \frac{\partial \omega_z}{\partial y}v = \frac{\beta}{Re} \left[ \frac{\partial^2 \omega_z}{\partial x^2} + \frac{\partial^2 \omega_z}{\partial y^2} \right] - \frac{\partial^2 T^{xy}}{\partial x^2} - \frac{\partial^2 T^{yy}}{\partial x \partial y} + \frac{\partial^2 T^{xx}}{\partial y \partial x} + \frac{\partial^2 T^{xy}}{\partial y^2}. \tag{31}$$

Therefore, the problem is to solve the system composed by Eqs. (4), (7)-(9) (30), (31). In the plan Poiseuille flow of a viscoelastic fluid problem, there are three types of boundary conditions used: inflow, outflow and wall boundary conditions. The inflow is specified according to the following conditions

$$u = U(y), \quad v = 0 \quad \text{and} \quad \mathbf{T} = 0.$$
 (32)

On wall boundaries, the no-slip condition and impermeability (u = 0, v = 0) are employed. At the outflow homogeneous Neumann condition are considered for both the velocity and the non-Newtonian contribution.

# 4.1 Base Flow

In this paper we study viscoelastic plane Poiseuille flow where x and y represent the streamwise and wall-normal directions. To calculate the base flow, it is assumed that all variables are dependent only on the y axis, except for the pressure whose gradient is constant in the x direction. The domain in the y direction is comprised between [-1,1].

For the Giesekus fluid the base flow was generated numerically by two-dimensional DNS code, without disturbances, and the simulations performed until the flow reached the steady state. Also, the variables for the base flow were taken in the middle of the channel.

#### 5. NUMERICAL METHOD

The system of Eqs. (1)–(3) is solved numerically in the domain as shown in Fig. 1. The calculations are performed on an orthogonal uniform grid, parallel to the wall. The fluid enters the computational domain at  $x=x_0$  and exits at the outflow boundary  $x=x_{max}$ . In this work, the infinitesimal disturbances behavior in the flow is investigated. Unsteady disturbances are introduced into the flow field using suction and blowing of mass at a disturbance strip on the walls, which is located between  $x_1$  and  $x_2$ .

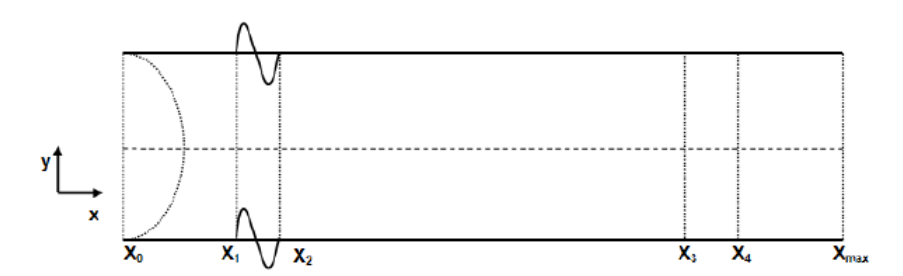


Figure 1. Definition of the computational domain for Poiseuille flow.

At first, when time t = 0, the flow is undisturbed, but from time t > 0, the disturbances are introduced in a disturbance strip near the inflow, by imposing the v velocity

$$v = Af(x)\sin(\omega_t t), \quad x_1 < x < x_2, \tag{33}$$

and

$$v = 0, \quad x \le x_1 \quad \text{or} \quad x \le x_2, \tag{34}$$

where A is a constant used to adjust the disturbances amplitude, f(x) is a 9th-order function. In the region located between  $x_0$  and  $x_1$  and  $x_3$  and  $x_4$  a buffer domain technique is implemented in order to avoid wave reflections from the inflow and outflow boundaries, respectively.

In the numerical method the time derivatives in the vorticity transport and the components of the non-Newtonian extra-stress tensor equations are discretized with a classical four step fourth-order Runge-Kutta integration scheme. The spatial derivatives are calculated using a high-order compact finite difference-schemes. The use of the adopted compact finite differences to estimate the first and second spatial derivatives requires the solution of tridiagonal linear systems. The numerical derivative approximations have 5th- and 6th-order of accuracy. The Poisson equation is solved using a multigrid Full Approximation Scheme (FAS).

Finally, with the purpose of eliminating numerical (spurious) oscillations, a filter is applied after the last Runge-Kutta step. This filter is applied in the vorticity component in the streamwise direction and in the non-Newtonian extra-stress tensor components.

We solve the system composed by Eqs. (4), (7)-(9), (30), (31) numerically by the application of the following algorithm:

- Step 1: Apply a step of the time integrator for the vorticity and the non-Newtonian extra-stress tensor.
- Step 2: Apply the functions responsible for the damping and relaminarization zones.
- Step 3: Introduce the suction and injection disturbances into the walls.
- Step 4: Calculate the right side of the Poisson equation, given by Eq. (30).
- Step 5: Calculate the v velocity by solving the Poisson equation [Eq. (30)].
- Step 6: Calculate the value of u velocity through Eq. (4).
- Step 7: Calculate the  $\omega_z$  vorticity through Eq. (31).
- Step 8: Calculate the components of the non-Newtonian extra-stress tensor through Eqs. (7)-(9).
- Step 9: Update the vorticity value  $\omega_z$  and the components of the non-Newtonian extra-stress tensor at the walls.
- Step 10: Apply the filter after the last sub-step of the time integrator.

The numerical simulation finishes when the desired wall clock time is reached.

#### 6. RESULTS

In this section, the numerical code verification is presented by comparing the present results with the Giesekus fluid and the results of the Oldroyd-B fluid. Also, the two-dimensional flow stability analysis between two parallel plates for Giesekus viscoelastic fluid is presented with the conformation tensor formulation. In this analysis, the influence of the dimensionless parameters  $\alpha$ ,  $\beta$  and Re was observed in the Giesekus viscoelastic fluid flow simulation.

## 6.1 Code Verification

In order to verify the actual DNS code implemented with the Giesekus fluid and the log and square root formulations applied to the conformation tensor, we consider the plane Poiseuille flow between two parallel plates. In this sense, numerical simulations were performed comparing the numerically generated base flow with the DNS code implemented with the Giesekus model, considering  $\alpha=0$  in the mathematical model with the conformation tensor formulation and the analytically generated base flow with the DNS code implemented with the Oldroyd-B model.

The parameters adopted for numerical simulation of the verification test were: the number of points in the streamwise and wall-normal directions are  $i_{max}=9049$  and  $j_{max}=249$ , respectively; the distance between two consecutive points in the x and y directions are  $dx=2\pi/(32\alpha_r)$  and  $dy=2/(j_{max}-1)$ , respectively, where  $\alpha_r$  is the real part of the wavenumber; the time steps per wave period are 248. Figure 2 is performed to verify the behavior of  $T^{xx}$  and  $T^{xy}$  non-Newtonian tensors and it is possible to notice that the behavior both formulations are in agreement.

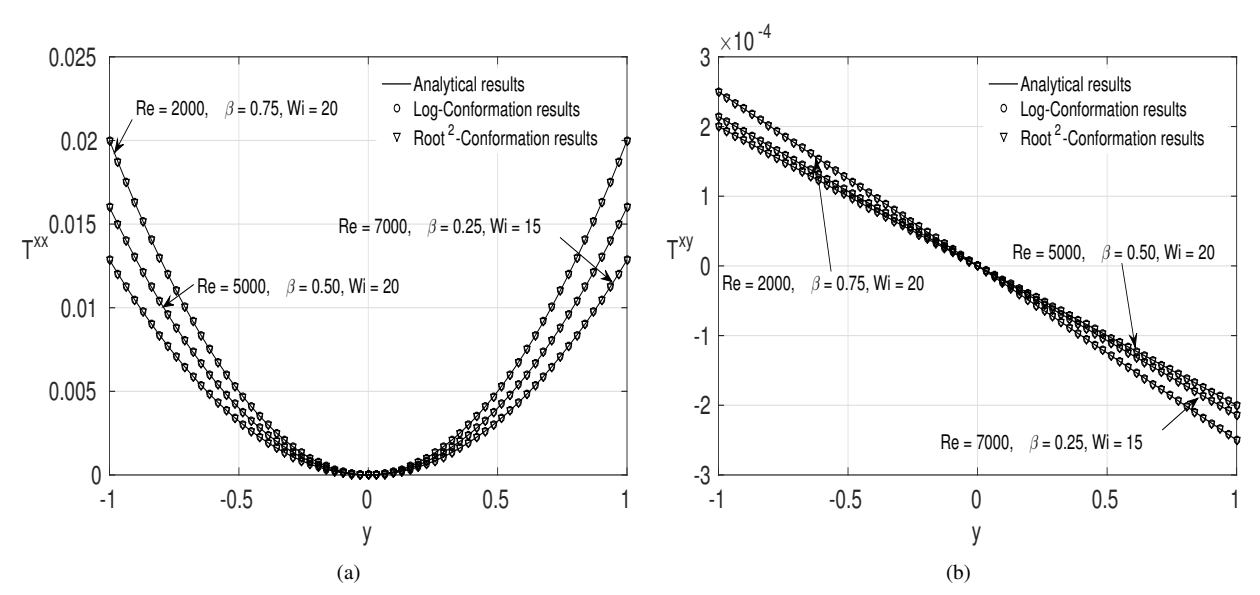


Figure 2. Numerical solutions obtained at the middle of the channel for Giesekus and Oldroyd-B fluids flows using different parameters.

# **6.2** The $\alpha$ Variation

Different numerical simulations are presented in order to verify the effect that the application of the kernel-conformation transformation has on maximum amplification rates. Simulations are performed by varying the non-dimensional parameters for viscoelastic fluid. Considering the viscoelastic Poiseuille flow using the Giesekus model, in this section, in particular, the effect of the  $\alpha$  parameter on numerical simulations is analyzed.

In these simulations two different values of Reynolds were considered: Re=2000 and 5000, three different values of  $\alpha=0.15,\,0.30$  and 0.45, two different Weissenberg values: Wi=5 and 80 and  $\beta=0.75$  fixed. The parameters adopted in the simulations performed here were: the number of points in the streamwise and wall-normal directions are  $i_{max}=505$  and  $j_{max}=249$ , respectively; the distance between two consecutive points in the x and y directions are  $dx=2\pi/(32\alpha_r)$  and  $dy=2/(j_{max}-1)$ , respectively, where  $\alpha_r$  is the real part of the wavenumber; time steps per wave period are 248, disturbance frequency  $\omega_t=0.2$ . The A parameter for adjusting the amplitude of Tollmien-Schlichting waves was  $1\times 10^{-4}$ .

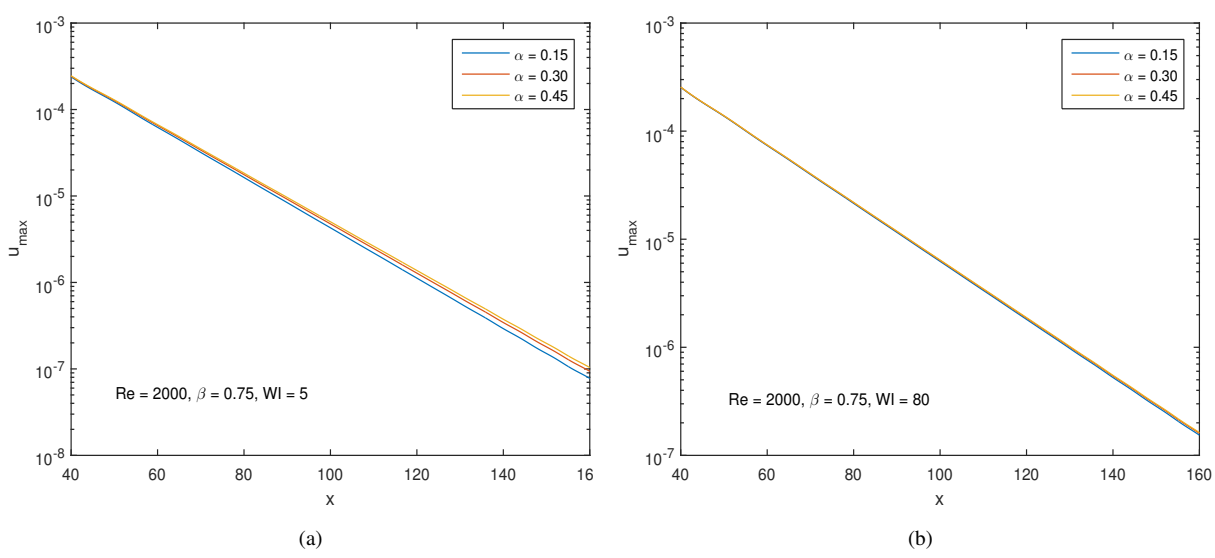


Figure 3. Maximum streamwise velocity disturbance development in the streamwise direction for different  $\alpha$  values, considering Re=2000: (a) Wi=5 and (b) Wi=80.

Figures 3, 4, 5 and 6 show the behavior of the maximum amplification rates for different dimensionless parameters in simulations in which Weissenberg number was set at Wi = 5 and Wi = 80. The simulations performed with the log-

conformation transformation can be seen in Figs. 3 and 4, considering the Reynolds number equivalent to 2000 and 5000, respectively. At the same time, Figs. 5 and 6 show the results obtained with the square root-conformation transformation to the same Re parameter variations.

Note that the application of kernel-conformation transformation ensured the flow stability, even in simulations with high Weissenberg numbers. In addition, the variation of the  $\alpha$  parameter showed that its increase became the flow less stable despite remaining stable, and that the greatest effects of this variation were noticed in simulations with bigger Reynolds number.

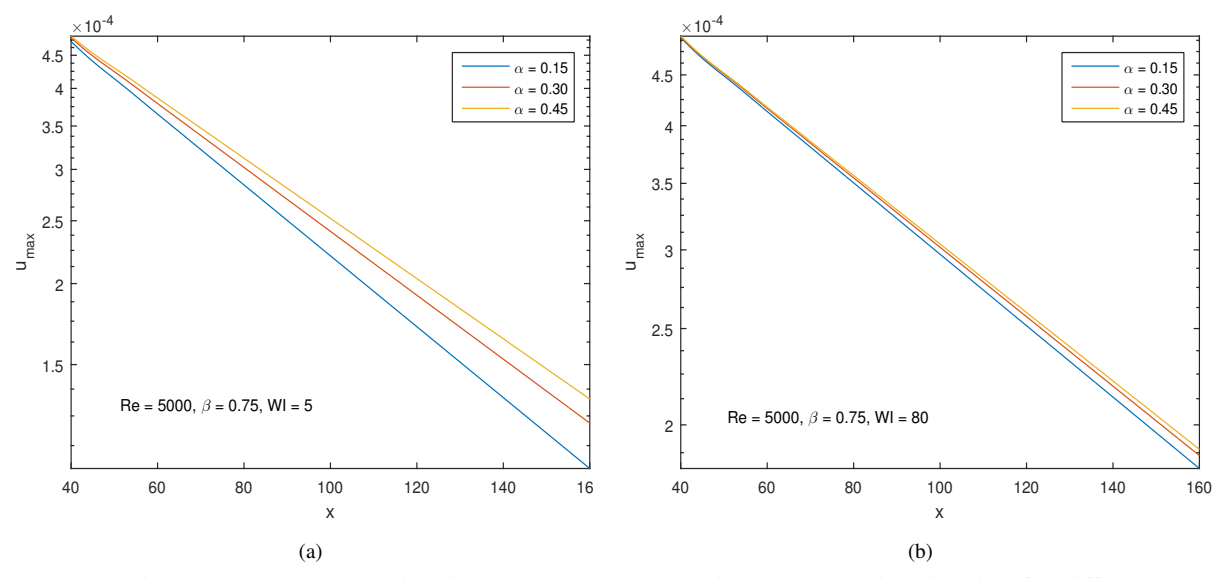


Figure 4. Maximum streamwise velocity disturbance development in the streamwise direction for different  $\alpha$  values, considering Re = 5000: (a) Wi = 5 and (b) Wi = 80.

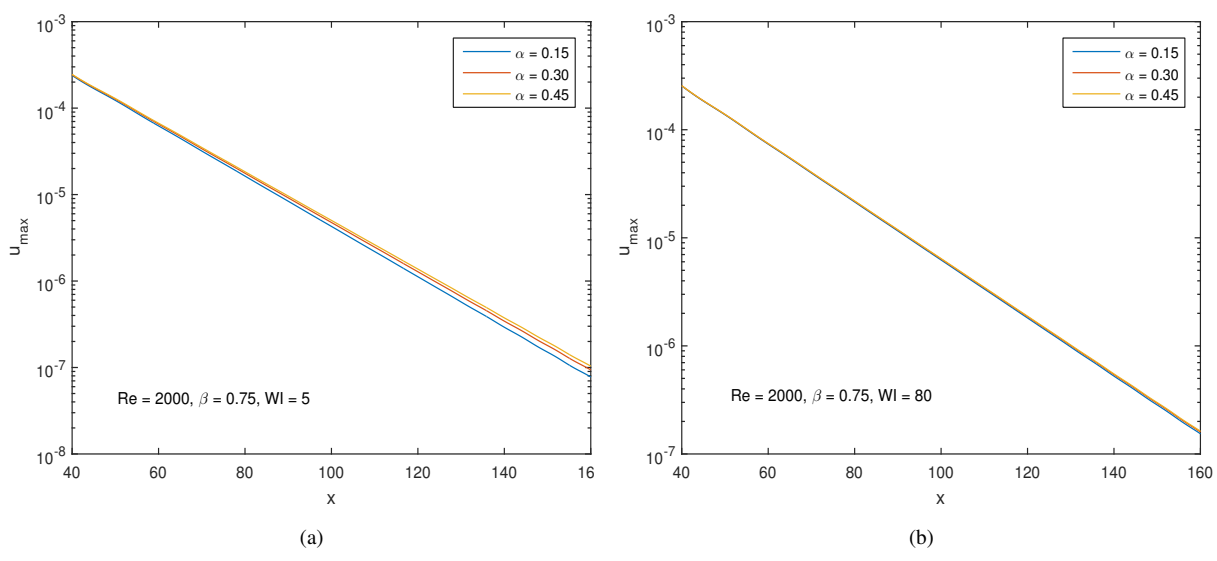


Figure 5. Maximum streamwise velocity disturbance development in the streamwise direction for different  $\alpha$  values, considering Re = 2000: (a) Wi = 5 and (b) Wi = 80.

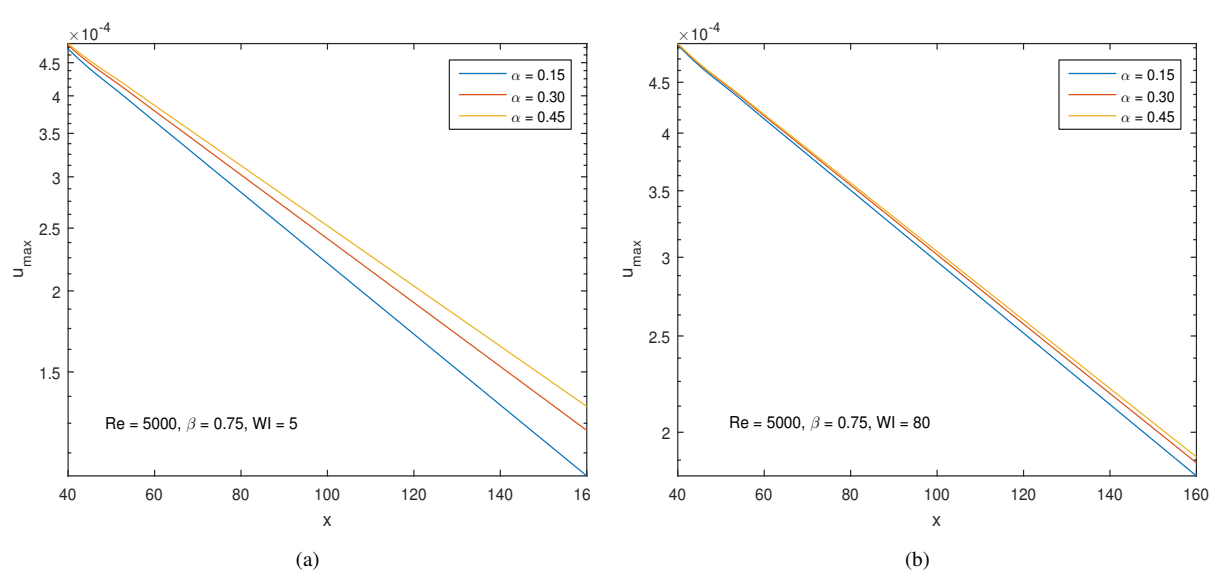


Figure 6. Maximum streamwise velocity disturbance development in the streamwise direction for different  $\alpha$  values, considering Re = 5000: (a) Wi = 5 and (b) Wi = 80.

# 6.3 Comparison between Log- and Square Root-Conformation Transformations

Now numerical simulations are presented to compare two kernel conformation transformations studied in this paper and for this, the maximum velocity amplification rates of u are observed.

In these simulations were considered the parameters: Re=2000,  $\alpha=0.45$  and  $\beta=0.50$ , with variation of the Weissenberg number. The other parameters are the same as those adopted in the previous simulations.

Figure 7 show that the application of the logarithmic and square root formulations in the conformation tensor was satisfactory in order to guarante the flow stability. Moreover, both formulations presented very similar behaviors.

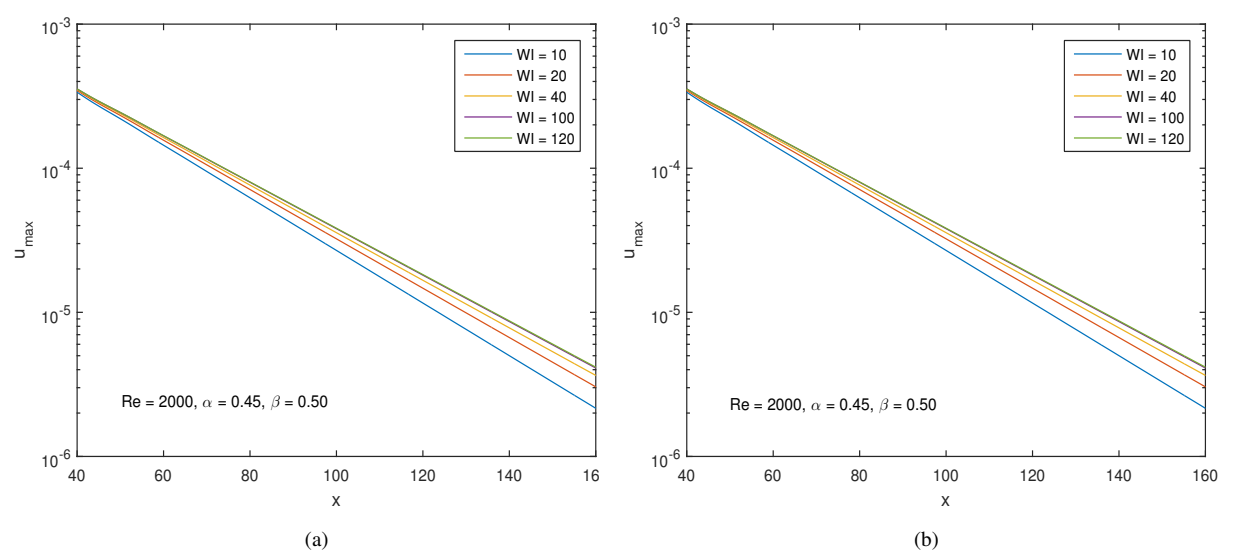


Figure 7. Maximum streamwise velocity disturbance development in the streamwise direction for different Wi values, considering Re = 2000: (a) Log-Conformation and (b) Square Root-Conformation.

# 7. CONCLUSIONS

This paper compares two different formulations of the same HWNP stabilization technique: the log- and square root-conformation transformation, considering Poiseuille flow stability for the Giesekus fluid, carried out by means Direct Numerical Simulation and the governing equations are written in a vorticity-velocity formulation.

In order to evaluate the maximum amplification rates, different dimensionless parameter values are tested for Newto-

nian and non-Newtonian fluid flows, with particular attention to Weissenberg number.

The results showed that an application of the kernel-conformation formulations in the numerical simulations guaranteed the flow stability in simulations with high Weissenberg numbers.

## 8. ACKNOWLEDGEMENTS

We thank the Coordination for the Training of Higher Education Personnel (CAPES) for the research grant we received during the development of this study.

#### 9. REFERENCES

- Afonso, A.M., Pinho, F.T. and Alves, M.A., 2012. "The kernel-conformation constitutive laws". *Journal of Non-Newtonian Fluid Mechanics*, Vol. 167, pp. 30–37.
- Balci, N., Thomases, B., Renardy, M. and Doering, C.R., 2011. "Symmetric factorization of the conformation tensor in viscoelastic fluid models". *Journal of Non-Newtonian Fluid Mechanics*, Vol. 166, pp. 546–553.
- Brandi, A.C., Mendonça, M.T. and de Souza, L.F., 2017. "Comparação de DNS e LST para o escoamento de Poiseuille do fluido Oldroyd-B". In 13º Congresso Ibero-americano de Engenharia Mecânica. Lisboa, Portugal.
- Fattal, R. and Kupferman, R., 2004. "Constitutive lows for the matrix-logarithm of the conformation tensor". *Journal of Non-Newtonian Fluid Mechanics*, Vol. 123, pp. 281–285.
- Fattal, R. and Kupferman, R., 2005. "Time-dependent simulation of viscoelastic flows at high Weissenberg number using the log-conformation representation". *Journal of Non-Newtonian Fluid Mechanics*, Vol. 126, pp. 23–37.
- Fortuna, A.O., 2012. *Técnicas Computacionais para Dinâmica dos Fluidos: Conceitos Básicos e Aplicações*. Editora da Universidade de São Paulo, São Paulo, 2nd edition.
- Giesekus, H., 1982. "A simple constitutive equation for polymer fluids based on the concept of deformation-dependent tensorial mobility". *Journal of Non-Newtonian Fluid Mechanics*, Vol. 11, pp. 69–109.
- Martins, F.P., Oishi, C.M., Afonso, A.M. and Alves, M.A., 2015. "A numerical study of the kernel-conformation transformation for transient viscoelastic fluid flows". *Jornal of Computacional Physics*, Vol. 302, pp. 653–673.
- Palhares Jr., I.L., 2014. *Decomposições Matriciais para Escoamentos Viscoelásticos Incompressíveis*. Ph.D. thesis, Universidade Estadual Paulista (Unesp), Presidente Prudente, Brazil.

#### 10. RESPONSIBILITY NOTICE

The authors are the only responsible for the printed material included in this paper.